APPLICATIONS PAPER

Precise Orthoimage Generation of Dunhuang Wall Painting

Yongjun Zhang, Zuxun Zhang, Mingwei Sun, and Tao Ke

Abstract

Wall painting plays an important role in the culture relics of the Mogao Caves in Dunhuang, P.R. China. A novel approach of generating a high-resolution orthoimage of the wall painting is proposed. Since the photographic object is nearly flat and also the forward overlap between adjacent images is smaller than 60 percent, the main difficulty to be resolved is the high correlation problem among the unknowns. Improved models of relative orientation and bundle adjustment with virtual constraints have been developed to resolve the high correlation problem. A Voronoi diagram of projective footprints is applied to automatically determine the mosaic lines of ortho-rectified images. The color quality of the generated orthoimage is improved through global minimization of the color differences among overlapped images. The experimental results show that the proposed approach has great potential for conservation of wall paintings with sub-millimeter to millimeter precision.

Introduction

The Mogao Caves in Dunhuang are the largest and oldest treasure house of Buddhist art in the world. There are about 500 caves where wall paintings are located, and they are the most important elements of the culture information of these relics. However, the Mogao Caves are being damaged by rock erosion and serious natural disasters as well as the negative effects of the increasing number of tourists at the site. Traditional protection methods, such as copy, photography, and videography, are not meeting the high precision protection requirement. It is now an urgent task to find the key high precision technologies that are capable of conserving the wall paintings.

In recent years, close-range photogrammetry and 3D laser scanning have been the most popular techniques for heritage conservation (Stylianidis *et al.*, 2005). Digital images have several advantages in photogrammetric applications, such as a mature working flow of data processing, a high potential for automation, and good geometric accuracy; while at the same time, the recent progress in terrestrial laser scanning technology now allows fast and efficient collection of 3D coordinates for cultural heritage preservation (Naci, 2007). A drawback of the laser scanner, however, is that it remains expensive. The data quality is also influenced by surface properties, and it is possible that there are millions of points even on a perfectly flat surface, which often result in oversampling (Remondino *et al.*, 2008). The latest laser scanner systems also cannot generate very high-resolution color images, which are very important for wall painting conservation. Independent image data acquisition has to be performed for the integration with laser scanner data. Precise registration between point clouds and images is the key problem to be resolved in order to get reasonable orthoimage. But there is no satisfactory technique available on the automatic registration between point clouds and optical images of planner objects.

However, high-resolution images acquired by digital cameras can be processed using image-based modeling techniques to survey and document cultural heritage (Altan *et al.*, 2004; Saloniaa, 2005). The image-based virtual Dunhuang Art Cave navigation system was developed by Lu and Pan (2000) using computer graphics and virtual reality technologies. Wei *et al.* (2003) virtually restored the color of ancient walls using artificial intelligence techniques. Ke *et al.* (2008) restored a wall painting with 5 to 10 mm accuracy using technologies of close-range photogrammetry and computer-based image processing. Different image processing algorithms and robust estimation methods are combined by Barazzetti *et al.* (2010) to obtain accurate locations and a uniform distribution of tie points in close range images. Close range orthoimage of 8 mm accuracy was achieved by Tsiligiris *et al.* (2003) with a pre-calibrated digital camcorder. There is no information in the literature about orthoimage generation of wall paintings with a sub-millimeter or even one millimeter level of geometric accuracy. However, in order to thoroughly digitize and protect the Buddhist wall paintings, the printed version produced with a 150 dpi printer should be the same size as the actual wall painting. That means the required ground sample distance (GSD) of the photographed images therefore must be better than 0.17 mm. The desired geometric accuracy is about one millimeter.

A new approach of precise orthoimage generation of Dunhuang wall paintings based on photogrammetric techniques is proposed in this paper. The general strategies for orthoimage generation and the data sources used for

Yongjun Zhang and Zuxun Zhang are with the School of Remote Sensing and Information Engineering, and the State Key Laboratory of Information Engineering in Surveying, Mapping and Remote Sensing, Wuhan University, No. 129 Luoyu Road, Wuhan, 430079, P.R. China (zhangyj@whu.edu.cn).

Mingwei Sun and Tao Ke are with and the State Key Laboratory of Information Engineering in Surveying, Mapping and Remote Sensing, No. 129 Luoyu Road, Wuhan, 430079, P.R. China.

Photogrammetric Engineering & Remote Sensing
Vol. 77, No. 6, June 2011, pp. 631–640.

0099-1112/11/7706–0631/$3.00/0

experiments are described in the next Section, followed by the detailed methodologies of orthoimage generation, including image matching, bundle adjustment with virtual constraints, ortho-rectification, and color correction. The experimental results of orthoimage generation are presented followed by further work recommendations.

General Strategy and Data Sources

General Strategy

The photogrammetric processing of close range images of quasi-planar wall paintings, such as image matching, bundle adjustment, ortho-rectification, and color correction, are the contents of the current work. The images used for experiments are acquired with a pre-calibrated digital camera fixed on a movable platform as shown in Figure 1. In order to eliminate outliers during image matching, automatic estimation of the relative orientation parameters is one of the most difficult problems, because they are highly correlated in the case of quasi-planar scenes and small forward overlap stereos. To avoid the high correlation problem and to detect gross mismatches, three parameters (by, bz, and κ) are used as unknowns of relative orientation firstly. Then ω and φ are treated as the weighted unknowns together with the above three parameters to detect the remaining subtle outliers. The precise conjugate point is acquired by a least-squares image matching within a local searching range predicted by the relative orientation parameters. The coordinates of the matched image points and measured ground control points (GCPs) are utilized as data sources of bundle adjustment. Moreover, the quasi-planar constraints of the projection centers are added into the bundle adjustment model. A digital surface model (DSM) is generated by filtering and interpolating the object points obtained through bundle adjustment. The original images are then ortho-rectified with the above generated DSM and the known exterior orientation parameters. Finally, the color quality of the ortho-rectified image is improved using color correction techniques.

Data Sources

The Research Institute of Dunhuang started the digitization and protection project of wall paintings several years ago. More than 20,000 images located in about 100 caves have already been obtained with 50 percent forward overlap and 50 percent sidelap a few years ago. These archived images are used for experimental purposes in this paper. The test wall painting used here is located on the south wall of an ancient cave and measures about 6 m long, 4 m wide, and 4 m high. The test wall appears to be a slightly bended plane, and the deflection at the top of the wall is only about 0.2 m. As shown in Figure 1, a mobile platform that can horizontally move along a fixed track utilizing gear wheels is set up in the cave for the convenience of photography. The track fixed on the ground is precisely aligned in parallel with the wall painting. A pre-calibrated Cannon EOS 1Ds Mark III digital camera with a focal length of 53 mm is mounted on the platform which can move up and down vertically. Under this hardware configuration, the projection centers of all the images are nearly coplanar, and the variations of all the projection centers against the ideal vertical plane are smaller than 0.02 m.

The object coordinate system is setup as follows: the origin is at the lower-left corner of the wall painting, the X-axis is horizontal and points to the right side, the Y-axis points upwards, and the Z-axis points outwards from the wall. The image format and physical pixel size of the camera are 5,616 $\times$ 3,744 pixels, and 0.0064 mm, respectively. The distance between the wall and the camera is approximately 1.0 m; thus, the GSD is about 0.13 mm. A total of 15 strips containing 298 images with about 50 percent forward overlap and 50 percent sidelap are obtained by the camera. The view directions of all images are parallel

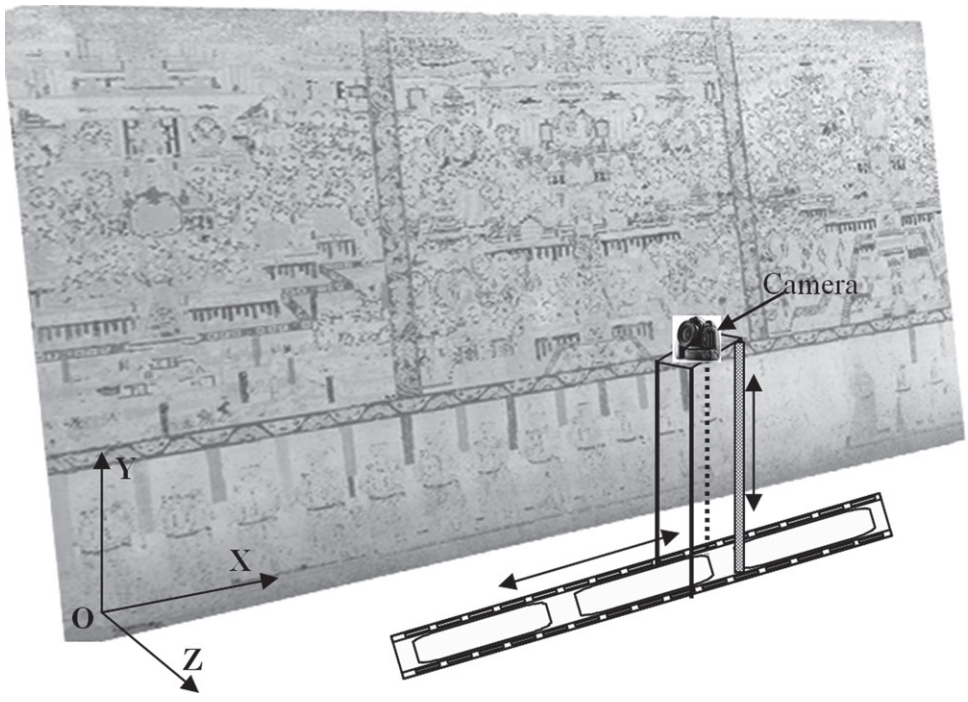

Figure 1. Photographic equipment and coordinate system of the test wall painting.

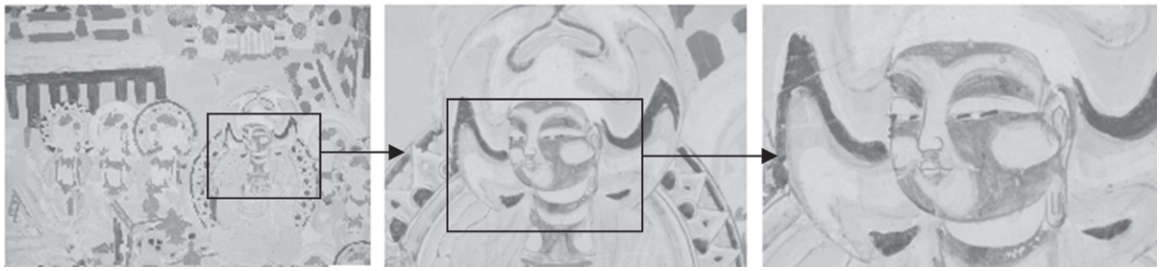

Figure 2. Photographed original image of the test wall painting: (a) full image with 1:25 resolution, (b) part of image with 1:8 resolution, and (c) part of image with 1:4 resolution.

to each other and perpendicular to the X-Y plane of the object coordinate system. Figure 2 shows one of the acquired images with resolutions of 1:25, 1:8, and 1:4. In order to evaluate the precision of the orthoimage generated by the proposed approach, 59 ground points are measured by an electronic total station. The planar and height accuracies of these points are about 1.0 mm and 2.0 mm, respectively. The 31 triangular-shaped points in Figure 3 are used as control points, while the other 28 square-shaped ones are check points for the bundle adjustment in the Experiments and Results Section.

Orthoimage Generation Methodology

Image Matching

Image matching is the prerequisite of many applications in computer vision and photogrammetry, including object recognition, motion tracking, bundle adjustment, and 3D information extraction. In this paper, an image matching process is also necessary to find conjugate points among adjacent images, which is composed of three steps: feature point extraction; area-based matching, and relative orientation.

Feature point extraction is the first step in all area-based image matching algorithms. There are several well known operators, such as Moravec, Forstner, and Harris (Moravec 1977; Förstner and Gülch 1987; Harris and Stephens, 1988). In this paper, the feature points of each image are first extracted with the Harris detector and then refined by the Förstner operator to obtain the necessary sub-pixel precision. Each image is divided into rectangular grids with a pre-defined grid size (e.g., 180 × 180 pixels). One feature point with the strongest interest value above a given threshold is extracted from each grid. About 600 feature points can be extracted from each of the images acquired by the aforementioned digital camera.

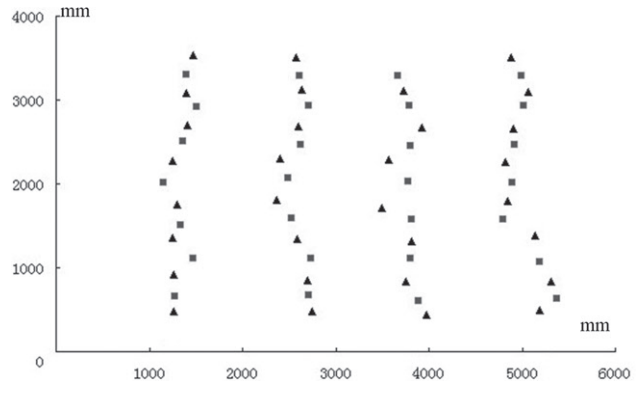

Figure 3. Distribution of control and checkpoints of the test wall painting.

A pyramid-based matching strategy, which is usually adopted by traditional image matching, is also used in this paper. Area-based matching with correlation coefficients can be performed as long as the approximate overlap and rotation angle of a stereo pair are available. The nominal overlap is sufficient for predicting the initial position of potential conjugate points for each feature point since the photographic object is nearly planar. Then, area-based image matching strategies, such as correlation coefficient and least-squares matching, are used to find precise conjugate points within a local range around the predicted position. For the purpose of connecting all of the stereo models, the matched image points in one stereo pair should be automatically transferred to all of the neighboring stereos, which can be accomplished by replacing the extracted feature points of the current stereo with the successfully matched conjugate points of the previous stereo.

In the traditional procedure of photogrammetry, relative orientation with five unknowns can be performed as long as five or more conjugate points are available. However, the relative orientation parameters (by and ω; bz and φ) are closely correlated because the wall painting is quasi-planar and the image overlap is less than 60 percent. Usually, the condition number of the normal matrix of relative orientation with natural terrain images is on the $5.0 \times e^7$ level, while the condition number of that with wall painting images is at least $5.0 \times e^9$ and sometimes larger than $1.0 \times e^{12}$. It is obviously an ill-posed problem that will result in inconsistent relative orientation solutions. Only the by, bz, and κ are used as unknowns to detect gross mismatches at the beginning of the relative orientation. Then, ω and φ are used as weighted unknowns in addition to the above three parameters to detect the remaining subtle outliers. In this case, the condition number of the normal matrix is on the $1.0 \times e^8$ level, which is much better than the traditional method. Least-squares adjustment with robust estimation technique is used to compute the unknowns of relative orientation. The calculated relative orientation parameters can be used to assist image matching by providing epipolar constraints. Figure 4 shows the automatically matched conjugate points of six stereo images. About 200 conjugate points are successfully matched between each stereo pair. The accuracy of image matching is usually better than 0.3 pixels since the least squares image matching strategy is applied. The white crosses in the images represent the conjugate points that pertain to images of a single strip while the black crosses represent conjugate points that pertain to images of two different strips.

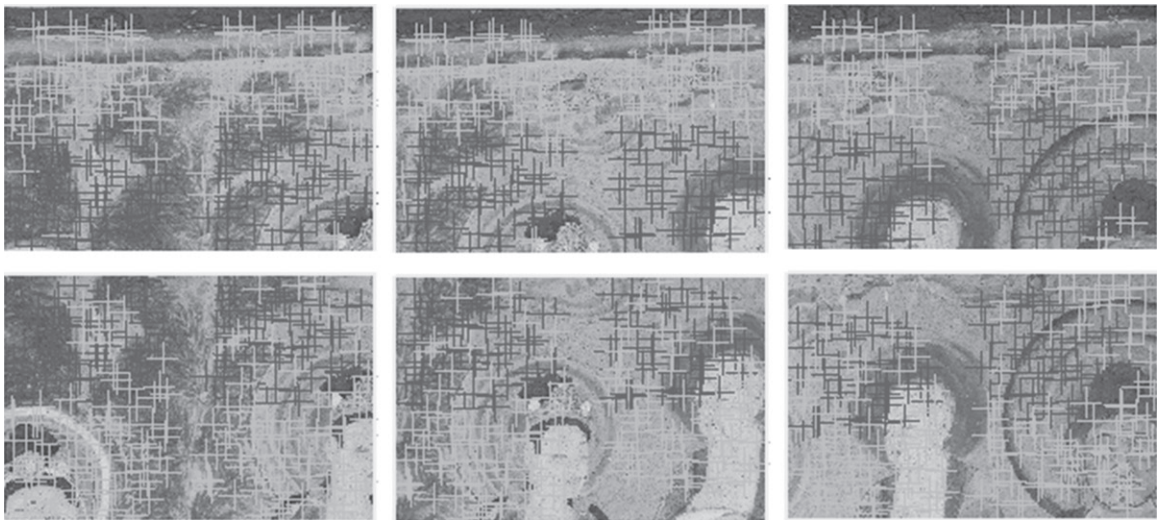

Figure 4. Automatically matched conjugate points among adjacent images.

Bundle Adjustment with Quasi-planar Constraints

Bundle adjustment is the key technology of geometric analysis and also a prerequisite of precise 3D information extraction. Collinearity equations are the basic mathematical model of bundle adjustment. However, the normal matrix of bundle adjustment is seriously ill-posed because the photographic object is quasi-planar, and moreover the overlap between adjacent images is only about 50 percent. Additional constraints must be considered in order to get reliable results from bundle adjustment. As previously described, all of the projection centers are nearly coplanar with about 0.02 m variation. This knowledge of the projection centers can be combined into the adjustment model to improve the geometric configuration of the normal equation. Note that the coplanar constraints of the projection centers cannot be used as strict conditions in combined bundle adjustment. They should be used rather as pseudo observations with 0.02 m *a priori* accuracy.

The interior parameters of the digital camera are calibrated just before photography, so self-calibration is not necessary for bundle adjustment. The collinearity equations are the basic mathematic model of bundle adjustment (Mikhail, *et al.*, 2001; Zhang *et al.*, 2008):

$$\begin{aligned} x - x_0 &= -f\frac{a_1(X-X_s)+b_1(Y-Y_s)+c_1(Z-Z_s)}{a_3(X-X_s)+b_3(Y-Y_s)+c_3(Z-Z_s)} \\ y - y_0 &= -f\frac{a_2(X-X_s)+b_2(Y-Y_s)+c_2(Z-Z_s)}{a_3(X-X_s)+b_3(Y-Y_s)+c_3(Z-Z_s)} \end{aligned} \quad (1)$$

where x and y are the observations, X, Y, and Z the coordinates of ground point, a_i, b_i, $c_i (i = 1,2,3)$ are the orientation matrix composed of rotation angles φ, ω, and κ where the Y-axis is taken as the primary axis, and $X_S, Y_S, Z_S, \varphi, \omega, \kappa, f, x_0, y_0$ are the exterior and interior parameters, respectively.

The same height constraints of the projection centers have the following form:

$$Z_{si} = Z_{sj} (i = 0,1,2 \ldots n, i \neq j) \quad (2)$$

where Z_{si}, Z_{sj} are the heights of the projection centers, and n is the number of projection centers. The combined bundle adjustment model is composed of Equations 1 and 2. The observation equations of the combined adjustment model have the following form:

$$\begin{matrix} V = BdT - l & P \\ V_{zs} = dZ_{si} - dZ_{sj} - W_{zs} & P_{zs} \end{matrix} \quad (3)$$

where B is the designed matrix of vector $dT = (dX, dY, dZ, dXs, dYs, dZs, d\varphi, d\omega, d\kappa)$, V and V_{zs} the correction vector of observations, l and W_{zs} constant items calculated by the approximate values of unknowns, and P and P_{zs} the corresponding weight matrix. The weight matrix is very important for bundle adjustment in order to obtain reliable solutions. The image matching precision is usually about 0.3 pixels. The initial weight of each image point is set to be 1.0, i.e., the unit weight root mean square error (or sigma naught) equals to 0.3 pixels in image space and 0.04 mm in object space since the GSD is 0.13 mm. The initial weights of pseudo observations are defined by their *a priori* accuracies against the unit weight variance. The *a priori* accuracies of the ground control points are 1.0 mm in planar and 2.0 mm in height, respectively, while the *a priori* accuracy of the heights of the projection centers is 0.02 m. Note that the weights of all observations are recalculated according to the iterated results during bundle adjustment.

Ortho-rectification and Color Correction

DSM, usually generated by image matching with extracted dense features, is an essential data source to generate orthoimages. In this paper, dense image matching is not necessary because the wall is quite smooth. DSM can be generated by filtering and interpolating the object points of aerial triangulation. Then, ortho-rectification can be performed image by image. The Voronoi diagram of the projective footprints is used to automatically generate mosaic lines of all the separately rectified orthoimages. As shown in Figure 5, the five white crosses are the planar positions of the projective centers, and the five corresponding polygons represent the automatically generated mosaic lines. Each closed polygon is filled with one ortho-rectified image. Therefore, the whole orthoimage of the wall painting is automatically generated after all of the polygons have been filled with corresponding orthoimage blocks.

Figure 5. Automatically generated mosaic lines of adjacent orthoimage blocks.

The illumination of photography is provided by special tubular lighting equipment. A standard color calibration target is used during image acquisition since the imagery is intended for conservation. However, the lighting conditions and the performance of the camera's auto-white balance function occasionally change slightly, and the photographed images often have different color hues, especially those belonging to different strips. These conditions will result in significant differences of color hues in the mosaicked orthoimage. Figure 6 shows an orthoimage block mosaicked by five adjacent images. Note that the lower part of Figure 6a has apparent color differences when compared to the upper part.

It is apparent that color correction must be performed to generate an orthoimage with uniform color hues. The basic idea of color correction is that the overlapped areas of adjacent images should have the same color hues. The first step of color correction is the calculation of the color hues of the overlapped areas among the adjacent images. Six correction parameters are then introduced for the three RGB channels of each image. Each channel has two correction parameters: the mean and the standard deviation of gray values. The color differences among the adjacent images are globally minimized by calculating the correction parameters of each image. Finally, the color of each ortho-rectified image is corrected according to the calculated parameters and the color-corrected images are mosaicked together as shown in Figure 6b. It is obvious that the proposed approach significantly improves the color quality.

Experiments and Results

Several sets of close range digital images and ground control points are used as sources of information for the experiments of the proposed approach. The experimental results are similar for all of the test data sets. Experimental results of image matching, bundle adjustment, digital orthoimage generation, and color correction of one of the wall paintings will be discussed in this Section.

Image Matching

Relative orientation is performed to calculate the five parameters and to detect the outliers, provided that five or more conjugate points are successfully matched. Then, an epipolar line, which can be calculated from the relative orientation

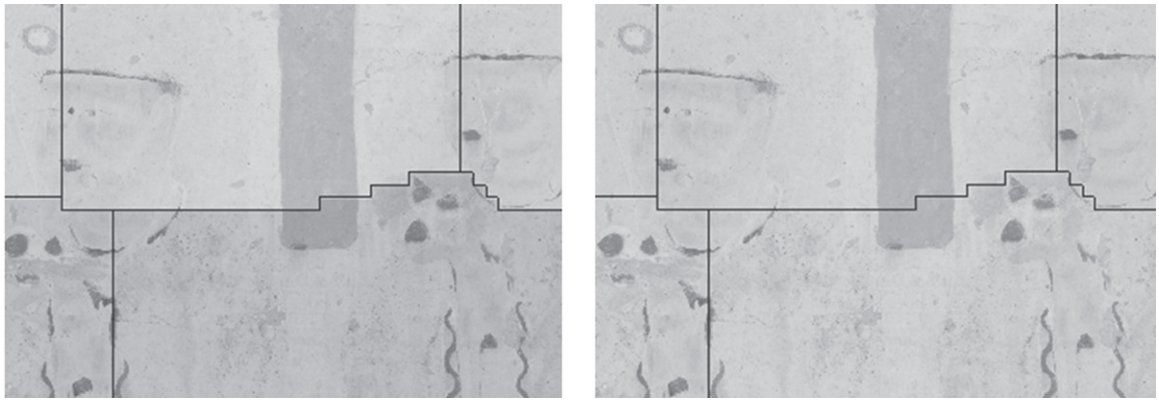

(a) (b)

Figure 6. Mosaicked orthoimage block before and after color correction: (a) before color correction, and (b) after color correction.

parameters, is used to reduce the searching range for image matching. There are usually 200 to 300 successfully matched conjugate points between each image pair with the proposed image matching strategy. The sigma naught of the relative orientation of both the forward overlap and sidelap stereos is usually in the range of 0.0015 mm to 0.0022 mm (i.e., one-fourth to one-third physical pixels). The crosses in Figure 7 are the automatically matched conjugate points of two forward overlap stereo pairs. As can be seen, all of the conjugate points are randomly distributed on the overlapped area. The conjugate points of the adjacent strip stereos are also very important for aerial triangulation because they can link different strips together. Figure 8 shows the automatically matched conjugate points of two sidelap stereo pairs. Similar to that of Figure 7, nearly no outliers remain among the conjugate points after relative orientation. The overall correctness rate of the matched conjugate points is higher than 98 percent, which means that less than two percent of them are possibly mismatched. These excellent results show that the proposed image matching algorithm is feasible to match image pairs of wall paintings.

The general overlaps and relative rotation angles between adjacent images can be calculated from the relative orientation parameters. The forward overlap of the test image data is in the range of 50 to 55 percent, while the sidelap is in the range of 48 to 52 percent. The maximum relative rotation angle between adjacent images is less than two degrees, which is the benefit of the photographic equipment shown in Figure 1.

Bundle Adjustment

Bundle adjustment with ground control points is performed in order to obtain precise exterior orientation parameters and thus generate a reasonable orthoimage of the wall painting for cultural heritage protection. 15,932 automatically matched conjugate points and 59 manually measured ground control points are used as data sources. As shown in Figure 3, 31 of the 59 points are used as GCPs, and the other 28 are checkpoints.

The interior orientation and lens distortion parameters are treated as known during bundle adjustment since the camera is precisely calibrated in advance. Two experiments of bundle adjustment are performed. The first is the traditional bundle adjustment without virtual constraints, while the second has virtual constraints as previously described. The unit weight root mean square (RMS) error of the two bundle adjustments are 0.0038 mm and 0.0033 mm, respectively. Error statistics of GCPs and checkpoints are shown in Table 1 and Table 2, respectively. As can be seen from Table 1, the RMS error of the planar position residues of the GCPs and checkpoints are both about 0.70 mm; while the RMS of the height residues of the check points is 4.06 mm, which is nearly two times of that of the GCPs. Furthermore, the maximum height residues of the GCPs and checkpoints are 4.86 mm and −7.77 mm, respectively. The result of the traditional bundle adjustment model is clearly deformed due to the poor geometric configuration. However, once the virtual constraints are combined into the bundle adjustment model, the result becomes quite acceptable. As shown in Table 2, the RMS errors of the planar position residues of the GCPs and checkpoints are slightly better than those of the first experiment, while the RMS errors of the height residues of the GCPs and check points are both at the 1.50 mm level. The maximum height residue is only about 2.10 mm, which is much better than that of the first experiment.

Although the achieved result of the second bundle adjustment is not comparable to the ground resolution of

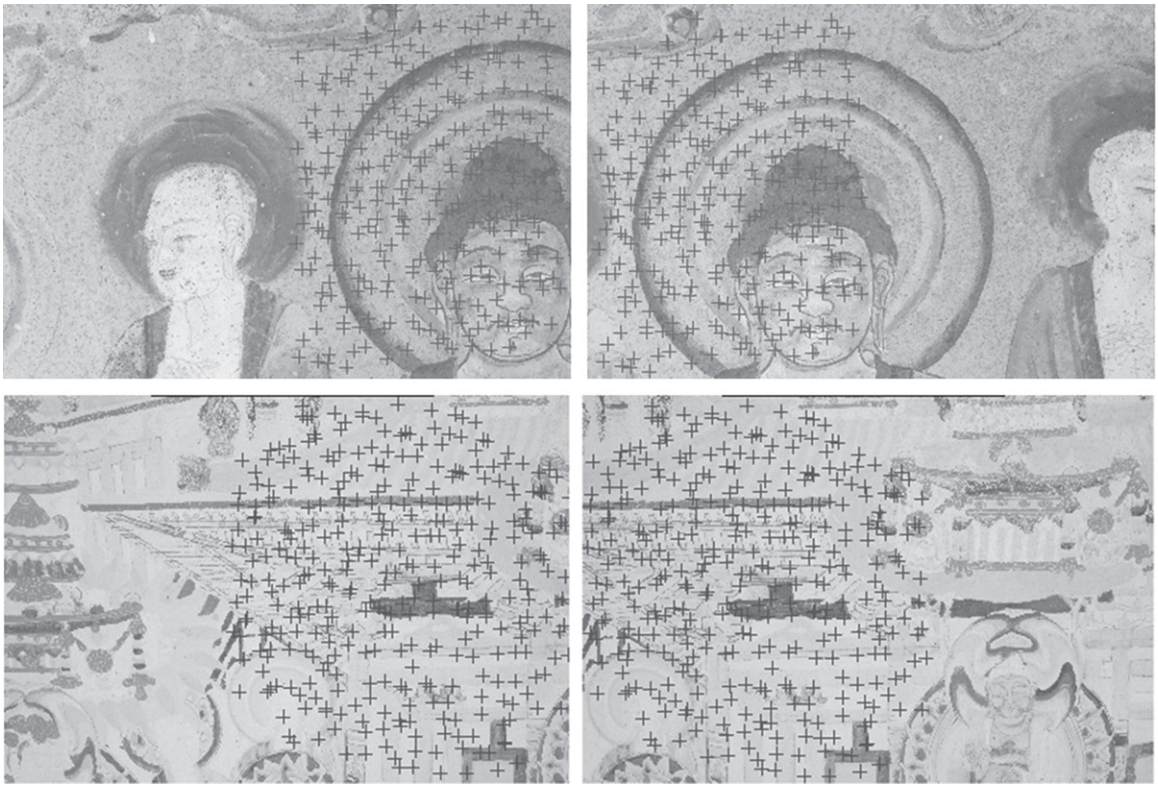

Figure 7. Matched conjugate points of two forward overlap stereo pairs.

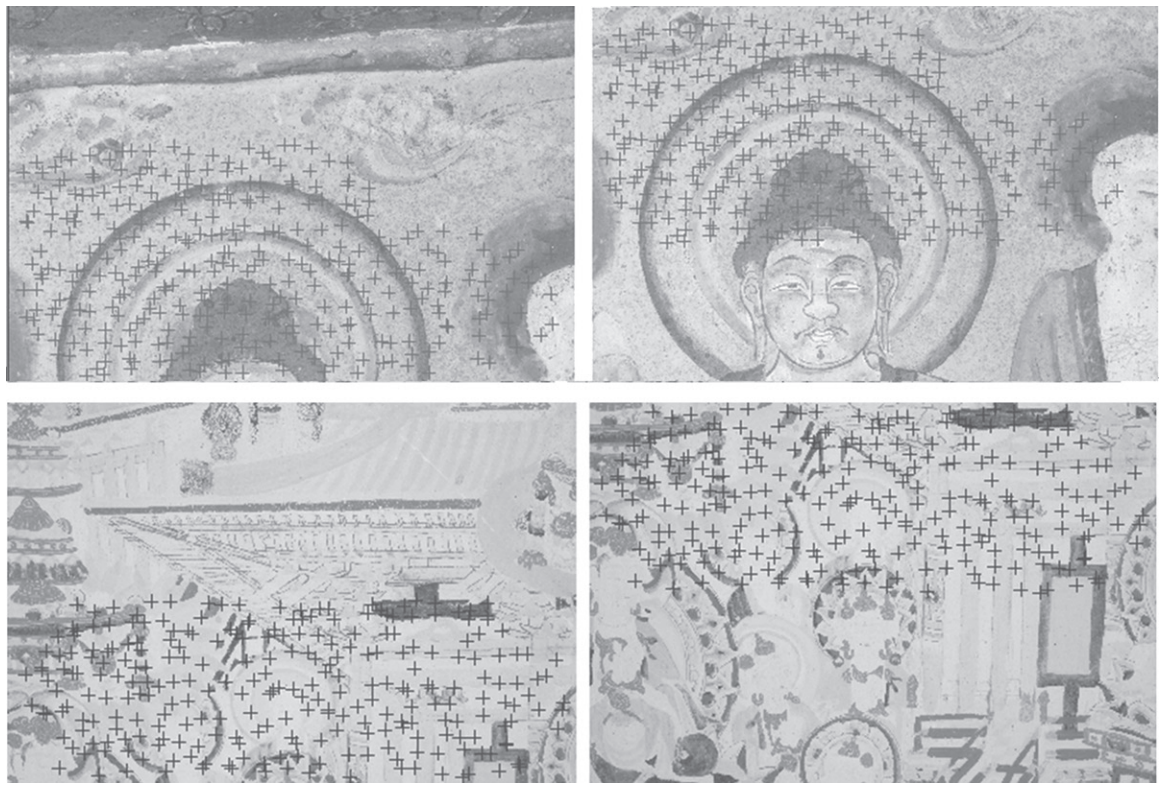

Figure 8. Matched conjugate points of two sidelap stereo pairs.

Table 1. Residues of Control and Checkpoints of Bundle Adjustment without Constraints (mm)

Item		RMS	Mean	Max/Min
Control Points	X	0.35	0.05	0.82
	Y	0.54	0.07	−2.03
	Z	2.12	0.16	4.86
Check Points	X	0.42	−0.11	0.77
	Y	0.60	0.12	1.36
	Z	4.06	−0.06	−7.77

Table 2. Residues of Control and Checkpoints of Bundle Adjustment with Constraints (mm)

Item		RMS	Mean	Max/Min
Control Points	X	0.27	0.03	0.60
	Y	0.49	0.04	1.05
	Z	1.24	0.06	2.05
Check Points	X	0.38	−0.05	−0.81
	Y	0.54	0.03	1.03
	Z	1.46	−0.04	2.09

imagery, it is reasonable since the control and checkpoints are measured by an electronic total station with a 1 mm + 1 ppm nominal accuracy of distance measurement. One can imagine that the bundle adjustment result will be significantly improved if more precise control and checkpoints are available.

Ortho-rectification and Color Correction

Once aerial triangulation is finished, a DSM can be generated by filtering and interpolating the obtained object point coordinates from aerial triangulation. As shown in Figure 9, the interpolated DSM of the test wall painting, which is produced by commercial software DPGrid (Zhang *et al.*, 2009), is quite smooth. Digital orthoimages can be obtained through ortho-rectification of the original images with the camera parameters and the interpolated DSM. The mosaic lines of all the ortho-rectified images are automatically calculated by the Voronoi diagram of the projective footprints. Plate 1a shows the mosaicked digital orthoimages of the test wall painting. As can be seen, there are apparent color differences among images of different strips in the lower part.

Two color correction parameters for each channel of a certain image are introduced to compensate for the color differences among the images. A total of 1,788 parameters are introduced for the 298 images. Each image is corrected by Wallis filtering (Mastin, 1985) with the estimated parameters of the desired mean and standard deviation. Plate 1b shows the final restored orthoimages of the test wall painting after color correction.

The precision of the generated orthoimage is verified by the GCPs and checkpoints that are used in bundle adjustment. The planar coordinates of the GCPs and checkpoints are interactively measured from the orthoimage and then compared with the ground truth. The RMS error of differences is smaller than 1.0 mm. In order to fully evaluate the precision of the generated orthoimage, an external verification is performed. The coordinates of seven randomly selected feature points on the actual wall painting are measured by the on-site electronic total station. The horizontal distances between an arbitrary two points are calculated by their world coordinates and compared with those measured from the orthoimage. The

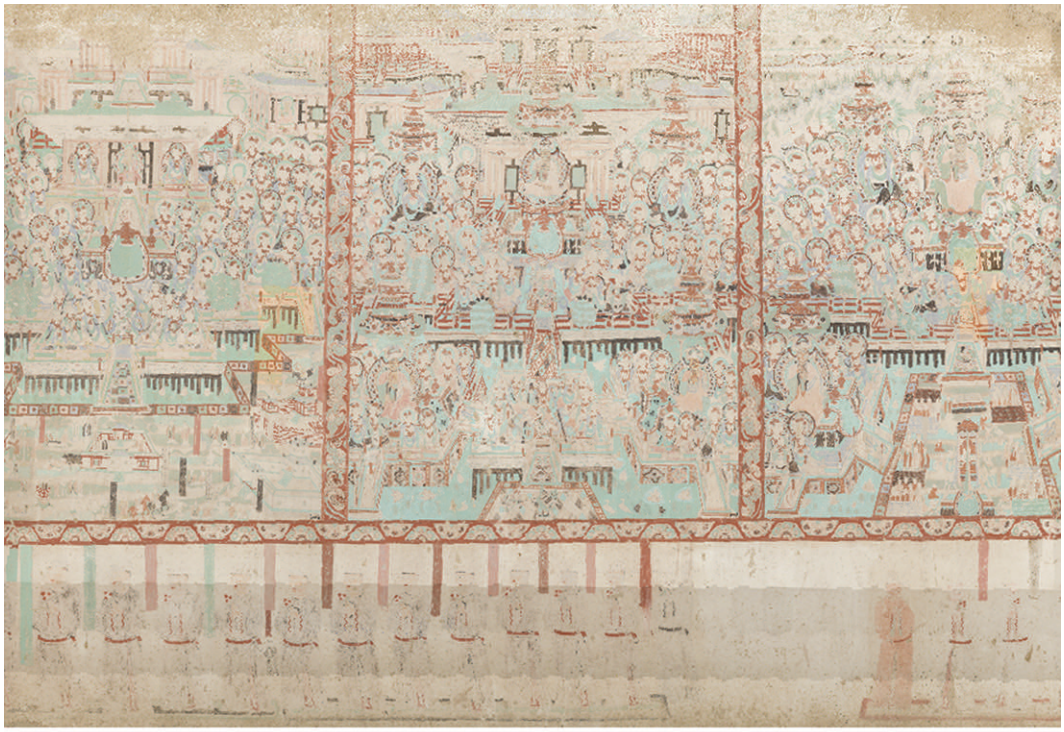

(a)

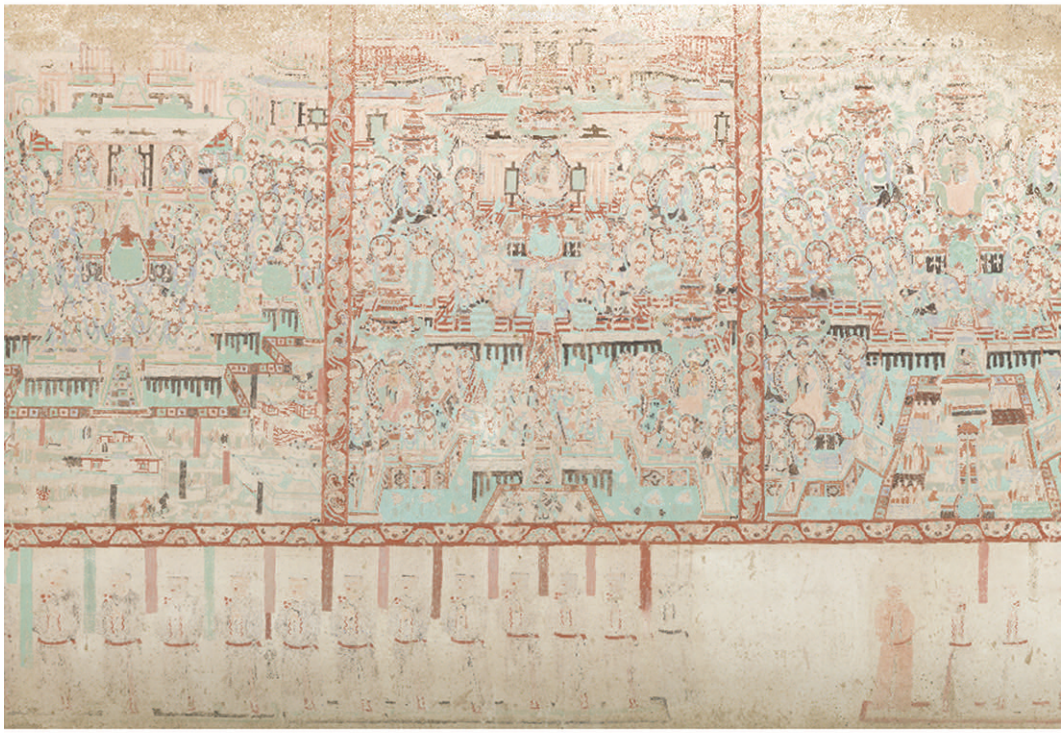

(b)

Plate 1. Digital orthoimage of the test wall painting: (a) before color correction, and (b) after color correction.

Figure 9. Digital surface model of the test wall painting.

maximum difference is also around 1.0 mm. These external checks further verify the geometric accuracy of the generated orthoimage. In fact, the internal geometric accuracy of the generated orthoimage should be on the sub-millimeter level because photogrammetry consistently generates an orthoimage with precision comparable to ground resolution. The millimeter level precision of the experiment is mainly determined by the accuracy of the GCPs. Further investigation is planned to verify this assumption in the near future.

Conclusions

A new approach of precise orthoimage generation for a quasi-planar object with close range images is discussed in this paper. The difficulties are that the photographic object is nearly flat, and the forward overlap is smaller than 60 percent, which will significantly influence the stability and reliability of the relative orientation and bundle adjustment. The pseudo observations of the coplanarity constraints of the camera translation parameters used in this paper are vital to improve the geometric configuration. The experimental results show that the proposed image matching strategy can automatically locate sufficient conjugate points from both the forward overlap and the sidelap image pairs. Pseudo observations of the constraints used in bundle adjustment significantly benefit the geometric configuration and thus improve the height precision. The geometric and color quality of the final orthoimage generated are satisfying for wall painting protection.

An objective color quality evaluation of the generated orthoimage is the main work planned in the near future. Improvement of the image acquisition equipment and measurement of the GCPs with higher accuracy also need to be investigated to generate more precise orthoimages of wall paintings.

Acknowledgments

This work is supported by the National Natural Science Foundation of China with Project No. 41071233, 40671157, the National Key Technology Research and Development Program with Project No. 2011BAH12B05, and the Program for New Century Excellent Talents in University with Project No. NCET-07-0645. I am very grateful also for the comments and contributions of anonymous reviewers and members of the editorial team.

References

Altan, M.O., T.M. Celikoyan, G. Kemper, and G. Toz, 2004. Balloon photogrammetry for cultural heritage, *Proceedings of The International Archives of the Photogrammetry, Remote Sensing and Spatial Information Sciences*, 12–23 July, Istanbul, Turkey, 35(B/5):964–968.

Barazzetti, L., F. Remondino, and M. Scaioni, 2010. Extraction of accurate tie points for automated pose estimation of close-range blocks, *Proceedings of The International Archives of the Photogrammetry, Remote Sensing and Spatial Information Sciences.* 01–03, September, Saint-Mandé, France, 38(3A): 151–156.

Cramer, M., 2007. The EuroSDR performance test for digital aerial camera systems, *Proceedings of Photogrammetric Week 2007*, pp. 89–106.

Förstner, W., and E, Gülch, 1987. A fast operator for detection and precise location of distinct points, corners and centres of circular features, *Proceedings of the ISPRS Inter-commission Workshop*, 02–04 June, Interlaken, Switzerland, pp. 149–155.

Harris, CG, and M.J. Stephens, 1988. A combined corner and edge detector, *Proceedings of the Fourth Alvey Vision Conference*, Manchester, UK, pp. 147–151.

Honkavaara, E., and A. Hogholen, 1996. Automatic tie point extraction in aerial triangulation, *Proceedings of the International Archives of the Photogrammetry and Remote Sensing*, 09–19 July, Vienna, Austria, 31(B/3):337–342.

Ke, C.Q., X.Z. Feng, and J.K. Du, 2008. 3D information restoration of the digital images of Dunhuang mural Paintings. *Proceedings of the International Archives of the Photogrammetry, Remote Sensing and Spatial Information Sciences*, 03–11 July, Beijing, China, 37(B/5):987–992.

Lu, D.M., and Y.H. Pan, 2000. Image-based virtual navigation system for art caves, *The International Journal of Virtual Reality*, 4(4):1–13.

Mastin, G.A., 1985. Adaptive filters for digital image noise smoothing: An evaluation, *Computer Vision, Graphics, and Image Processing*, 31(1):103–121.

Mikhail, E.M., J.S. Bethel, and J.C. McGlone, 2001. *Introduction to Modern Photogrammetry*, *John Wiley & Sons, Inc.*, 496 p.

Moravec, H.P., 1977. Towards automatic visual obstacle avoidance, *Proceedings of the 5th International Joint Conference on Artificial Intelligence*, Massachusetts, p. 584.

Naci, Y., 2007. Documentation of cultural heritage using digital photogrammetry and laser Scanning, *Journal of Cultural Heritage*, 8(4):423–427.

Remondino, F., S. El-hakim, E, Baltsavias, M. Picard, and L. Grammatikopoulos, 2008. Image-Based 3D modeling of the erechteion, acropolis of Athens, *Proceedings of the International Archives of the Photogrammetry, Remote Sensing and Spatial Information Sciences.* 03–11 July, Beijing, China, 37(B/5): 1083–1091.

Rizzi, A., F. Voltolini, S. Girardi, L. Gonzo, and F. Remondino, 2007. Digital presentation, documentation and analysis of paintings, monuments and large cultural heritage with infrared technology, digital cameras and range sensors, *Proceedings of 21st International CIPA Symposium on Anticipating the Future of the Cultural Past.* 01–06 October, Athens, Greece, unpaginated CD-ROM.

Saloniaa, P., A. Negri, L. Valdarnini, S. Scolasticoa, and V. Bellucci, 2005. Quick photogrammetry systems applied to documentation of cultural heritage: The example of Aosta Romen city wall. *Proceedings of 20th International CIPA symposium on International Cooperation to Save the World's Cultural Heritage*, 26 September – 01 October, Torino, Italy, unpaginated CD-ROM.

Stylianidis, E., P. Patias, C. Liapakis, V. Balis, and G. Philotheou, 2005. Visualization of frescos by means of photogrammetry and laser scanning, *Proceedings of 20th International CIPA Symposium on International Cooperation to Save the World's Cultural Heritage*, 26 September – 01 October, Torino, Italy, unpaginated CD-ROM.

Tsiligiris, E., M. Papakosta, C. Ioannidis, and A. Georgopoulos, 2003. Close range orthoimage using a low cost digital camcorder, *Proceedings of 19th International CIPA Symposium on*

New Perspectives to Save Cultural Heritage, 30 September – 04 October, Antalya, Turkey.

Wei, B.G., Y.H. Liu, and Y.H. Pan, 2003. Using hybrid knowledge engineering and image processing in color virtual restoration of ancient murals, *IEEE Transactions on Knowledge and Data Engineering.* 15(5):1338–1343.

Zhang, Z.X., Y.J. Zhang, and J.Q. Zhang, 2008. Photogrammetric modeling of linear features with generalized point photogrammetry, *Photogrammetric Engineering & Remote Sensing*, 74(9):1119–1129.

Zhang, Z.X., Y.J. Zhang, T. Ke, and D.H. Guo, 2009. Photogrammetry for first response in Wenchuan earthquake, *Photogrammetric Engineering & Remote Sensing*, 75(5):510–513.

(Received 02 December 2010; accepted 28 January 2011; final version 15 February 2011)